Hindawi
Journal of Nanomaterials
Volume 2022, Article ID 7112174, 10 pages
https://doi.org/10.1155/2022/7112174

Research Article

Modification of Silicone Hydrogel Contact Lenses for the Selective Adsorption of Ofloxacin

Wenke Xiao,[1,2] Xiaojuan Zhang,[1,3,4] Lingyun Hao,[1,3] Yuan Zhao,[1,3] Qing Lin,[1,3] Zhao Wang,[1,3] Wenli Song,[1,3] and Dong Liang[1,3]

[1]*School of Material Engineering, Jinling Institute of Technology, Nanjing 211169, China*
[2]*College of Energy Materials and Chemical Engineering, Hefei University, Hefei 230601, China*
[3]*Nanjing Key Laboratory of Optometric Materials and Technology, Nanjing 211169, China*
[4]*National Special Superfine Powder Engineering Research Center, Nanjing University of Science and Technology, Nanjing 210094, China*

Correspondence should be addressed to Xiaojuan Zhang; zxj831005@hotmail.com

Received 8 September 2021; Revised 2 December 2021; Accepted 7 December 2021; Published 1 February 2022

Academic Editor: Zehra Durmus

It is essential to design multifunctional contact lenses for selective recognition and utilization of the eye drop ofloxacin (OFL). Modified silicone hydrogel (MSL) contact lenses were firstly synthesized via ultraviolet curing by using (hydroxymethyl)methyl aminomethane, polydimethylsiloxane, methacryloxypropyl terminated polydimethylsiloxane, and *N*,*N*-dimethylacrylamide as monomers and N-vinyl-2-pyrrolidinone (NVP) as a modifier. The synthesized MSL contact lenses were characterized via Fourier transform infrared spectroscopy, scanning electron microscopy, and contact angle and mechanical property tests. The results showed that compared with silicone hydrogel (SL) contact lenses, the MSL contact lenses had a more porous structure and good swelling and mechanical properties. The molecularly imprinted polymer/ofloxacin-modified silicone hydrogel (MIP/OFL-MSL) contact lenses were firstly synthesized via free radical polymerization, using ofloxacin (OFL) as the template molecule. Moreover, compared with chlorogenic acid and myricetin molecule, the MIP/OFL-MSL contact lenses exhibited an adsorption capacity for OFL that reached 2.86 mg/g. The antibacterial test showed that the MIP/OFL-MSL contact lenses displayed an inhibition ring size of 15.2 mm and 17.8 mm for *Staphylococcus aureus* and *Escherichia coli*, respectively.

1. Introduction

The incidence of visual problems and eye diseases is increasing with the rapid development and growing popularity of electronic products. Ofloxacin (OFL) is a third-generation quinolone, and OFL eye drops are largely used in the treatment of eyelid inflammation, conjunctivitis, and other eye diseases [1–3]. However, the bioavailability of eye drops is low, and eye drops are difficult to circulate for a long time [4]. One of the biggest factors that lead to the bioavailability of topical drugs is the residence time of drugs [5]. The concentration of active ingredients in eye drops on the eye surface is diluted and eliminated due to the continuous turnover of tears. This condition limits the absorption of drugs by the eyes [6]. It was reported that emulsion solvent evaporation was used for fabricating nanoparticles to encapsulate OFL to enhance drug effectiveness by increasing ocular drug penetration and absorption [7]. Antibacterial results were obtained for silver core@silica mesoporous@OFL, proving the efficacy and synergetic effect of the OFL [8].

Corneal contact lens drug delivery systems can effectively improve the eye residence time of drugs by preventing drug dilution and excretion [9]. In vivo studies have confirmed the effectiveness of OFL-loaded lenses in reducing bacterial load to clinically insignificant levels and OFL–vitamin E-loaded lenses in reducing bacteria on the cornea to undetectable levels [10]. An efficacy study on a rabbit model demonstrated equivalent healing effect with OFL-loaded microemulsion-soaked contact lenses compared with frequent high-dose eye drop therapy [11]. Coating solid lipid

nanoparticles with chitosan and polyethylene glycol augments the ocular bioavailability of OFL by increasing transcorneal permeation and enhancing mucoadhesion strength [12]. Compared with poly-hydroxyethyl methacrylate contact lenses, contact lenses with 2.5 mol% polyacrylic acid exhibited enhanced loading of OFL and neomycin by 18 and 53 times, respectively. Charge interactions between comonomers and the drug were considered primary factors in the substantial increase in drug loading [13].

Silicone materials are widely used in the development and research of high-oxygen permeable contact lenses [14] due to their good mechanical properties, biocompatibility, excellent chain flexibility, large volume of siloxane group, and large diffusion coefficient of oxygen [15, 16]. Considering that the moisture content of pure silicone material is zero, the prepared contact lenses are easy to attach to the cornea due to their hydrophobicity, making the user uncomfortable. Therefore, we developed silicone hydrogel (SL) contact lenses that combine the excellent oxygen permeability of silica gel and the excellent hydrophilicity of conventional hydrogel materials [17–19].

Molecular imprinting is a new detection and separation technology developed by simulating the specific recognition between an enzyme and a substrate or an antigen and an antibody in an organism [20]. Molecular imprinting technology has two key components. The first is the template, which matches the size, shape, or functional groups of the target drug molecules. The second is the functional monomer, which produces noncovalent interactions with the template in a prepolymer mixture [21]. To increase complementarity between polymer and template molecules, a specific shape or generic functional area is created inside. For example, an α-cyclodextrin-based porous polymer was molecularly imprinted with dibutyl phthalate, which can be used for its selective removal [22]. Molecular imprinting was performed directly on bacterial cellulose to avoid the use of synthetic materials in the sustained release of quercetin, which was used as the template molecule. The molecularly imprinted bacterial cellulose exhibited approximately 1.6 times higher capability to bind to quercetin than the nonimprinted bacterial cellulose [23]. A molecular imprinting system offers a switchable function by using the Diels–Alder reaction between the furan group and phenyl maleimide [24].

For molecularly imprinted systems, the production of a drug's macromolecular framework in the process of polymer synthesis has been proven to be capable of improving the drug loading of contact lenses and considerably accelerating the controlled drug release effect. Tieppo et al. proved that ketotifen fumarate (Mw = 425), a small molecular weight therapeutic agent, can be successfully extended in vivo from molecularly imprinted contact lenses [25]. Compared with those of topical drops and drug immersion lenses, the mean residence time and bioavailability of ketotifen fumarate are significantly increased. This finding indicates that molecular imprinting provides an exciting and reasonable engineering strategy for sustained release. Evidently, imprinted contact lenses are a highly promising and more effective drug delivery system than eye drops.

In this study, SL contact lenses were synthesized via ultraviolet (UV) curing, and surface modification of the SL contact lenses by NVP was firstly performed. Molecularly imprinted polymers (MIPs) that are capable of the selective recognition of OFL were synthesized through free radical polymerization. Furthermore, the selective adsorption and antibacterial properties were tested.

2. Experiment

2.1. Materials. Methacryloxymethyltris(trimethylsiloxy)silane (Tris), *N*-vinyl-2-pyrrolidinone (NVP), ethylene glycol dimethacrylate (EGDMA), and diphenylphosphine oxide (TPO) were obtained from Shanghai Aladdin Bio-Chem Technology Co., Ltd. Polydimethylsiloxane and methacryloxypropyl terminated (DMS) were from Meryer (Shanghai) Chemical Technology Co., Ltd. *N*,*N*-Dimethylacrylamide (DMA) and polyvinyl pyrrolidone (PVP) were purchased from Sinopharm Chemical Reagent Co., Ltd. Ethanol and methanol were procured from Nanjing Chemical Reagent Co., Ltd. OFL and oleic acid were obtained from Shanghai McLean Biotechnology Co., Ltd. 2,2′-Azobis(2-methylpropionitrile) (AIBN) was from Shanghai Sihewei Chemical Co., Ltd. Methacrylic acid (MAA) was purchased from Yonghua Chemical Technology Co., Ltd. Acetic acid was acquired from Xilong Chemical Co., Ltd. Phosphate-buffered saline (PBS) solution (pH = 7.4) was obtained from Wuhan Boster Biological Technology, Ltd.

2.2. Modification of Silicone Hydrogel Contact Lenses (MSL). The synthesis of modified silicone hydrogel contact lenses (MSL) is shown in Figure 1. First, 1.7 mL of Tris, 0.4 mL of DMS, and 0.8 mL of DMA were mixed. Then, a mixture of 0.18 mL of NVP and 15 μL of EGDMA was added. NVP was added to increase water content. EGDMA was used as a cross-linking agent. Subsequently, 0.3 mL of ethanol and 8 mg of TPO were added, and the mixture was stirred for 5 min to mix it evenly. The reaction solution was poured into a polytetrafluoroethylene mold. After UV irradiation for 40 min, MSL contact lenses were obtained and soaked in 30% ethanol solution overnight to remove unreacted residues. For comparison, we also synthesized SL contact lenses without adding NVP. The composition of MSL and SL contact lenses in this study is exhibited in Table 1.

2.3. Synthesis of the MIP/OFL-MSL Contact Lenses. The synthesis of the MIP/OFL-MSL contact lenses is shown in Figure 2. To combine molecular imprinting with MSL contact lenses, 0.5 g of MSL contact lenses was further modified by adding 0.1 mL of oleic acid, and 0.4 mL of EGDMA cross-linker was added. Then, 0.1 mmol of OFL and 34.5 μL of MAA were mixed and shaken at 25°C for 10 min to obtain the preassembled solution. The MSL contact lenses were mixed with the preassembled solution. The prepolymerization complex was formed via covalent chemistry and achieved after ultrasonication for 30 min. Subsequently, 0.04 g of PVP was dissolved in 10 mL of 80% ethanol solution. The preassembled solution and 1 mg of AIBN were added. The polymerization reaction was kept at 60°C in a

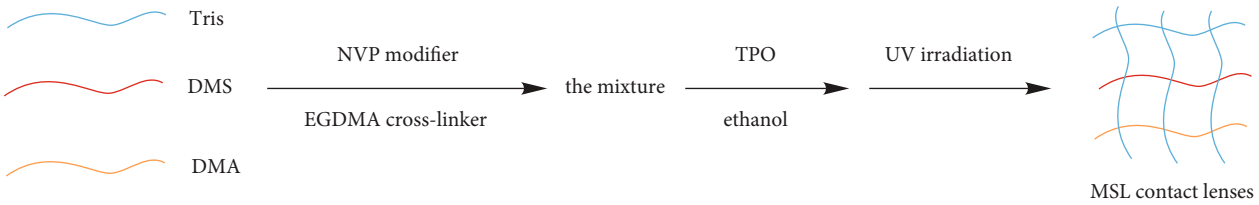

Figure 1: Synthesis diagram of modified silicone hydrogel contact lenses (MSL).

Table 1: The composition of MSL and SL contact lenses in this study.

Sample	Tris	DMS	DMA	NVP	EGDMA	Ethanol	TPO
MSL contact lenses	1.7 mL	0.4 mL	0.8 mL	0.18 mL	15 μL	0.3 mL	8 mg
SL contact lenses	1.7 mL	0.4 mL	0.8 mL	0	15 μL	0.3 mL	8 mg

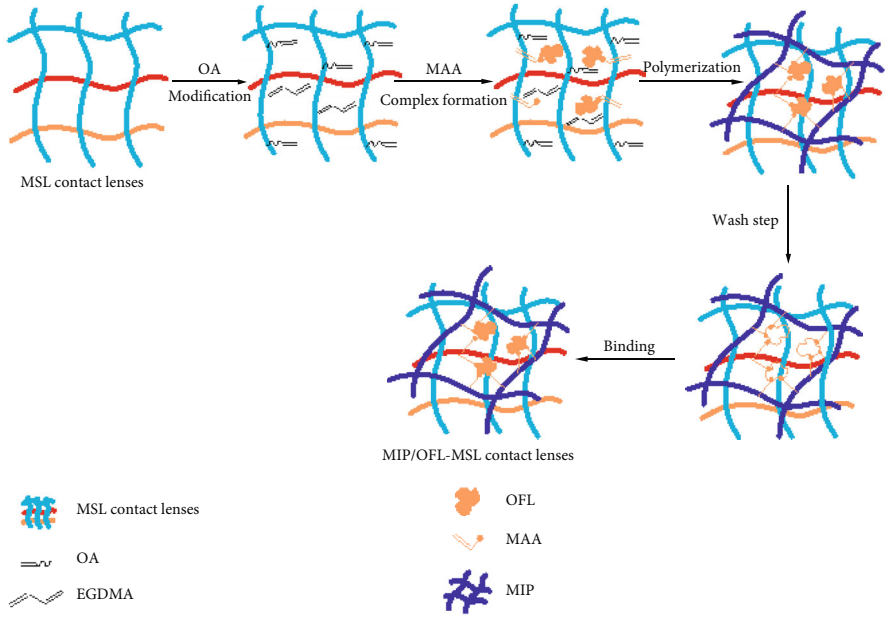

Figure 2: Synthesis diagram of molecularly imprinted polymer/ofloxacin-modified silicone hydrogel contact lenses (MIP/OFL-MSL).

water bath for 24 h with continuous stirring (300 rpm). The molecule imprinted polymer network was formed. The molecularly imprinted polymer/ofloxacin-modified silicone hydrogel (MIP/OFL-MSL) contact lenses were washed several times with methanol/acetic acid solution until no drug molecules were detected and then washed three times with deionized water. Then, the MIP/OFL-MSL was washed where the original OFL template could be removed and rebounded. For comparison, we also synthesized molecularly imprinted polymer/modified silicone hydrogel (MIP-MSL) contact lenses without adding OFL. The composition of MIP/OFL-MSL contact lenses in this study is exhibited in Table 2.

2.4. Determination of the Infrared (IR) Spectrum, Scanning Electron Microscopy (SEM) Morphology, and Contact Angles of the Contact Lenses. SL, MSL, and MIP/OFL-MSL contact lenses were freeze dried and then were measured by Fourier transform infrared spectroscopy (FTIR) using a Thermo NICOLET iS10 spectrometer. The morphology of the contact lenses was observed via SEM using a Hitachi Model S-4800 microscope. The contact angles of the SL contact lens films were tested using a contact angle meter (Kruss-DSA25).

2.5. Moisture Rate of the Contact Lenses. The weight of SL and MSL contact lenses was recorded as W_{a1} and W_{a2}. The contact lenses were put into the oven at 37°C. Then, the mass was recorded as W_{b1} and W_{b2} every half an hour till their weight remained unchanged. The moisture rate (MR) can be calculated by

$$\mathrm{MR} = \frac{W_a - W_b}{W_a} \times 100\%. \quad (1)$$

Table 2: The composition of MIP/OFL-MSL contact lenses in this study.

Sample	MSL	OA	EGDMA	OFL	MAA	PVP	Ethanol
MIP/OFL-MSL	0.5 g	0.1 mL	0.4 mL	0.1 mmol	34.5 μL	0.04 g	10 mL

2.6. Swelling Properties of the Contact Lenses. Swelling rate (SR) was measured in PBS (pH = 7.4) at different temperatures: (a) 25°C and (b) 37°C. The MSL and SL contact lenses (2 cm × 2 cm) were dispersed in 100 mL of PBS solution at different temperatures for 24 h to reach the maximum swelling equilibrium. The SR of the SL contact lens films was determined using [26].

$$\mathrm{SR} = \frac{W\mathrm{s} - W\mathrm{q}}{W\mathrm{q}} \times 100\%, \quad (2)$$

where W_q is the initial mass of the sample and W_s is the mass of the sample after swelling for 24 h.

2.7. Air Permeability. Three centrifuge tubes were prepared with 20 mL distilled water. MSL contact lenses were put in the first tube, and their mass was recorded as W_{x1}. SL contact lenses were put in the second tube, and their mass was recorded as W_{x2}. The third tube was the blank control, and its mass was recorded as W_c. Then, three centrifuge tubes were placed in the oven at 37°C for 24 h. Then, the mass of three tubes were recorded as $W_{x1'}$, $W_{x2'}$, and $W_{c'}$, respectively. The air permeability (AP) of contact lenses was calculated with

$$AP = \frac{Wx - Wx'}{Wc - Wc'} \times 100\%, \quad (3)$$

2.8. Transmittance of the Contact Lenses. The transmittance of MSL and SL contact lenses was analyzed by using an ultraviolet spectrophotometer (UV1101M054). The contact lenses with the thickness of about 1.8 mm were pasted on the transparent surface of the colorimetric plate. The transmittance of the contact lenses was measured in the wavelength range of 300-750 nm.

2.9. Mechanical Properties of the Contact Lenses. The tensile strength and elongation at break of the MSL and SL 5contact lenses were tested using a universal testing machine (Instron, Model 5943), and the crosshead speed was 10 mm/min at room temperature. The MSL and SL contact lenses were prepared with dimensions of 20 mm × 12 mm × 1.8 mm.

2.10. Selective Adsorption of the Contact Lenses. 0.13 g MIP-MSL contact lenses were placed in 30 mL chlorogenic acid (CHA) and myricetin (MYR) aqueous solution with a structure similar to OFL, respectively. The adsorbent was stirred at 25°C by using a shaker, and the absorbance of the drug solution was measured every 2 h. The adsorption amount was calculated. The selective adsorption properties of the MIP-MSL contact lenses were studied.

0.13 g MIP-MSL and 0.13 g MSL contact lenses were placed in 30 mL OFL aqueous solution. The adsorbent was oscillated at 25°C on a shaking table. The absorbance of OFL solution at 286 nm was measured using a UV spectrophotometer. Adsorption capacity was calculated in accordance with the change in solution concentration before and after adsorption by using

$$Q = \frac{(C_0 - C_t)V}{m}. \quad (4)$$

Q represents the adsorption capacity of OFL by the contact lenses per unit mass (g). C_0 is the initial concentration of the solution (mg/mL). C_t is the concentration of the solution after adsorption (mg/mL). V is the volume of OFL solution (mL). m is the weight of the contact lenses (g).

2.11. Antibacterial Study of the Contact Lenses. The antibacterial activity of the contact lenses was evaluated against *Staphylococcus aureus* and *Escherichia coli*. Muller–Hinton agar was used as the culture medium [27]. The MIP-MSL and MIP/OFL-MSL contact lenses were sterilized and cut into a circle sample with a diameter of 0.5 cm. The MIP-MSL and MIP/OFL-MSL contact lenses and the drug-sensitive papers (streptomycin and cefixime) were spread on the culture medium, which was evenly coated with bacteria. After 24 h of culture, the antibacterial effect was measured based on the inhibition zone surrounding each sample.

3. Results and Discussion

3.1. FTIR Analysis. The FTIR spectra of the SL, MSL, and MIP/OFL-MSL contact lenses are shown in Figure 3. In Figure 3 a, the peak at 3340 cm^{-1} was assigned to an -OH bond [28]. The band around 2960 cm^{-1} could be attributed to the stretching vibration of C–H from silicone. The peak at 1720 cm^{-1} can be ascribed to the C=O bond. The deformation vibration at 1640 cm^{-1} was -NH_2 [29]. The stretching vibration of Si–CH_3 was at 1260 cm^{-1} [30]. The peak of the -Si–O–Si- characteristic band in Tris appeared at 1040 cm^{-1} [31]. The band at 840 cm^{-1} can be ascribed to the C–H out-plane bending vibration of the benzene ring, and the peak at 802 cm^{-1} was the characteristic absorption band of Si–C stretching vibration. In Figure 3 b, the alkane chain C–H peaks in the NVP grafted onto the MSL contact lenses appeared at 2960 cm^{-1}. The C=O bond peak at 1720 cm^{-1} was stronger, proving that NVP was chemically cross-linked with a monomer [32] and that NVP-modified MSL was synthesized. As shown in Figure 3 c, the decrease in the intensity around 3340 cm^{-1} was due to the interaction of the template with the monomer in MIP/OFL-MSL [33]. These results proved that the molecularly imprinted MSL contact lenses were synthesized.

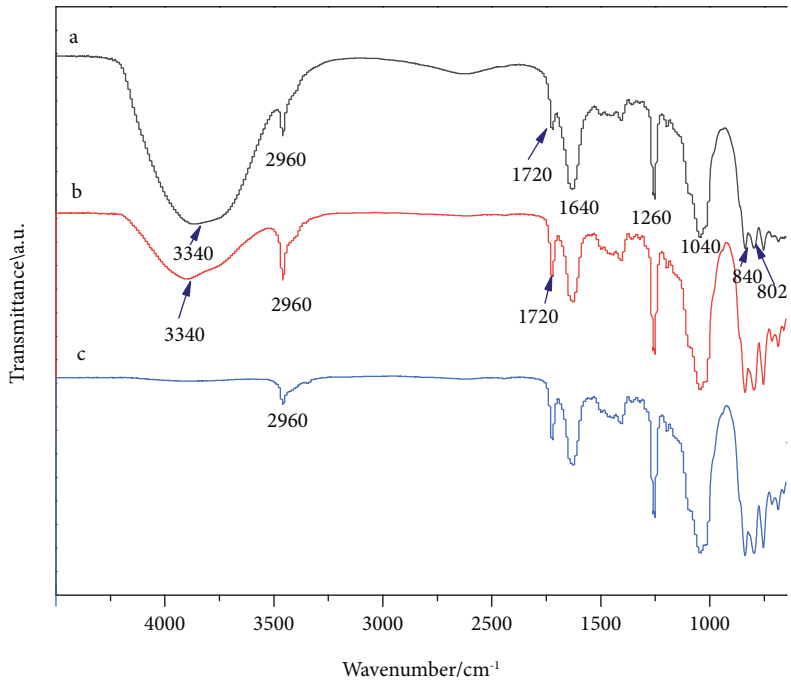

Figure 3: FTIR spectra of (a) SL, (b) MSL, and (c) MIP/OFL-MSL contact lenses.

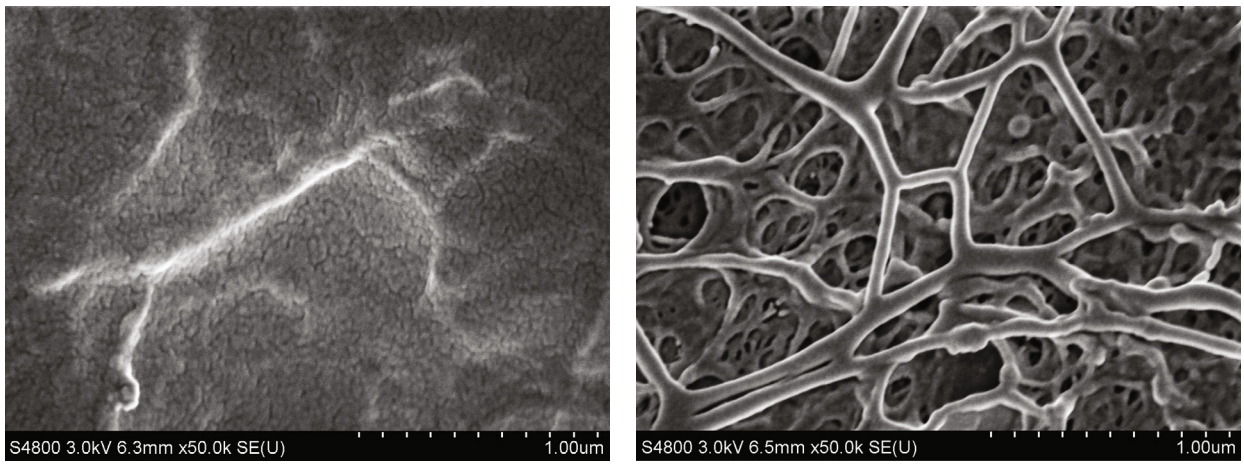

(a) (b)

Figure 4: SEM images of the (a) SL and (b) MSL contact lenses.

3.2. SEM Analysis. The morphology of the SL and MSL contact lenses was observed via SEM, as shown in Figure 4. One apparent difference between the SL and MSL contact lenses was that the surface of the MSL contact lenses (Figure 4(a)) formed large cavities, whereas that of the SL contact lenses (Figure 4(b)) was smooth. After modification, the surface of the MSL contact lenses had porous structure, which was ascribed to the fact that adding hydrophilic components to a system can increase hydrophilicity and improve porosity [31]. This type of porous structure plays an important role in swelling kinetics [34]. Freeze-drying can maintain the porous structure of the MSL contact lenses, improving the porosity of the MSL contact lenses [35].

3.3. Contact Angle Analysis. The contact angles of the SL and MSL contact lenses were $97.5° \pm 0.9°$ and $61.1° \pm 1.2°$, respectively. The contact angle of the SL contact lenses was higher than that of the MSL contact lenses, indicating that the addition of NVP during polymerization successfully improved the hydrophilicity of the MSL contact lenses.

3.4. Moisture Rate Analysis. Figure 5 presents the moisture rate of the SL and MSL contact lenses over time. At 200 min, the moisture rate of the SL and MSL contact lenses reached 11.9% and 17.2%, respectively. At 600 min, the moisture rate of the SL and MSL contact lenses were 19.9% and 25.2%, respectively. The moisture rate of both contact

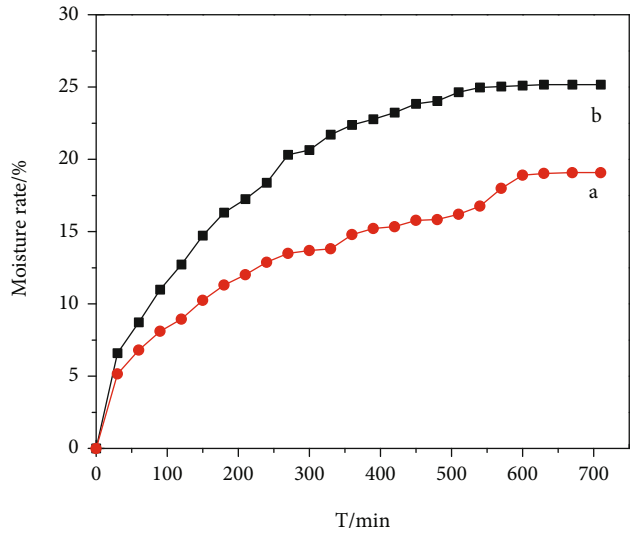

Figure 5: Moisture rate of the (a) SL and (b) MSL contact lenses.

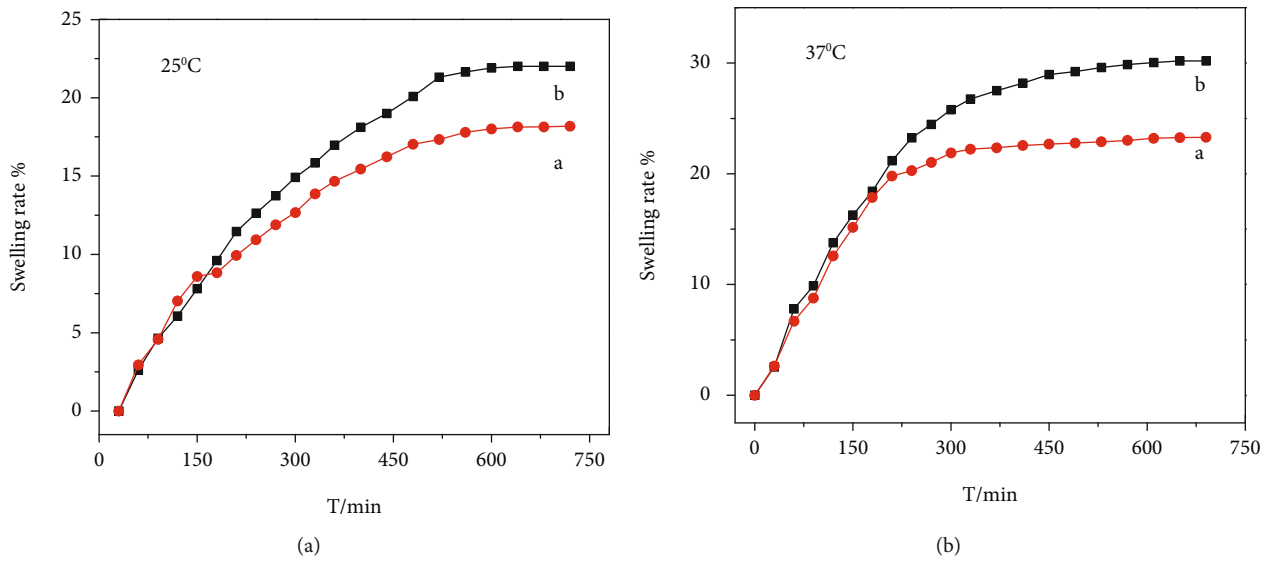

Figure 6: SR of the (a) SL and (b) MSL contact lenses at different temperatures: (a) 25°C and (b) 37°C.

lenses remained stable. Compared with that of the SL contact lenses, the moisture rate of the MSL contact lenses was higher, indicating that the MSL contact lenses exhibited good moisturizing properties.

3.5. Swelling Property Analysis. Figure 6 shows the SR of the SL and MSL contact lenses in PBS (pH = 7.4) at different temperatures: (a) 25°C and (b) 37°C. In Figure 6(a), the equilibrium SR of the MSL contact lenses at 25°C reached 22.0% at 700 min, which was higher than that of the SL contact lenses at 25°C (18.2%). As shown in Figure 6(b), the SR of the SL and MSL contact lenses at 37°C was 23.3% and 30.2% at 700 min, respectively. The increase in SR in the MSL contact lenses may be attributed to the binding between NVP and the SL contact lenses, which is responsible for higher cross-links and more porous structure. The higher swelling of MSL affects the imprinting of the polymer, and it was due to the fact that it blocks the imprinted sites and opens up the surface of polymer leading to unspecific binding [36].

3.6. Air Permeability Analysis. To avoid damage to the eyes caused by lack of oxygen, the materials of corneal contact lens should exhibit good air permeability. The air permeability of the SL and MSL contact lenses is labeled in Table 3. The MSL contact lenses demonstrated an air permeability of approximately 23.7%, which was higher than that of the SL contact lenses (18.5%). The air permeability of the MSL contact lenses was significantly higher than that of the SL contact lenses. The addition of NVP during polymerization improved the water content and helped the water vapor bind to the MSL contact lenses which resulted in passing through the MSL contact lenses.

Table 3: Air permeability of the SL and MSL contact lenses.

Sample	W_x (g)	$W_{x'}$ (g)	W_c (g)	$W_{c'}$ (g)	AP (%)
SL contact lenses	12.25	11.81	11.88	9.51	18.5
MSL contact lenses	12.34	11.78	11.88	9.51	23.7

3.7. Transmittance Analysis. In accordance with the international standard, the light transmittance of uncolored contact lenses should be more than 90% [37]. The wavelength range of visible light is 390–780 nm [38]. As shown in Figure 7, the transmittance of the MSL contact lenses (~45%–65%) was evidently better than that of the SL contact lenses (~47%) in the visible light range. Compared with commercial contact lenses, the central thickness of silicone hydrogel contact lenses was 0.08–0.20 mm. Therefore, the transmittance of the MSL contact lenses should be corrected. The thickness of the contact lenses was 0.2 mm, and the transmittance of the MSL contact lenses at a wavelength of 550 nm was determined. The transmittance of the synthesized MSL contact lenses was corrected via the IR spectrum. The equation used is as follows:

$$Ta = 100 - \frac{0.2(100 - T)}{d}, \quad (5)$$

where T is used to measure the transmittance of hydrogel, d is the measured actual thickness of the contact lenses, and T_a is the corrected transmittance. The transmittance of the SL and MSL contact lenses was 94.19% and 95.06%, respectively. Evidently, the SL and MSL contact lenses exhibited good transmittance, which meets the requirements of contact lens materials.

3.8. Mechanical Property Analysis. The mechanical properties of the SL and MSL contact lenses are presented in Figure 8. As exhibited in Figure 8 a, the tensile strength and elongation at break of the SL contact lenses were 0.552 MPa and 103.28%, respectively. Figure 8 b shows that the tensile strength and elongation at break of the MSL contact lenses were 0.649 MPa and 117.75%. It can be concluded that the synthesized MSL contact lenses were more flexible and elastic, which had better mechanical properties. It was due to the fact that the addition of NVP increased the cross-linking of contact lenses which provided the better mobility of the hydrogel.

3.9. Selective Adsorption Analysis. As shown in Figure 9(a), the adsorption capacity of the MIP-MSL contact lenses for OFL increased steadily with time (Figure 9(a) A) and the adsorption capacity was high (~2.86 mg/g). Figure 9(a) B shows that the adsorption of the MIP-MSL contact lenses for MYR exhibited no evident regularity and reached 1.34 mg/g after 25 h. As shown in Figure 9(a) C, the adsorption of CHA by the MIP-MSL contact lenses was gradual and the adsorption capacity was extremely low (~0.01 mg/g). By contrast, it was found that the MIP-MSL contact lenses exerted certain selectivity for OFL. And the structure of OFL (A), MYR (B), and CHA (C) is exhibited in

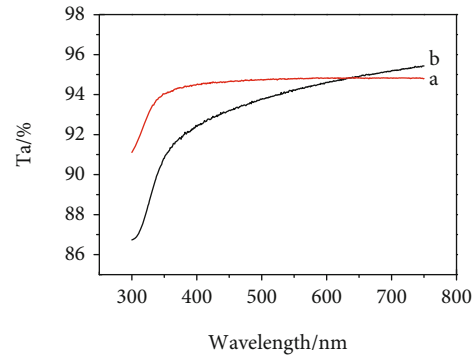

Figure 7: Transmittance curve of the (a) SL and (b) MSL contact lenses.

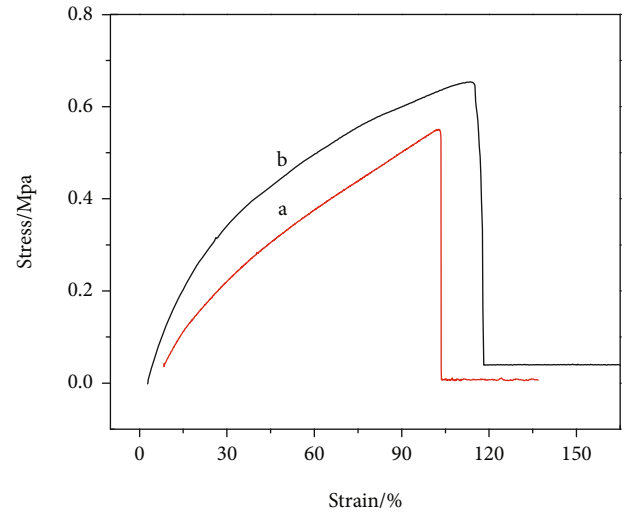

Figure 8: Mechanical properties of the (a) SL and (b) MSL contact lenses.

Figure 9(c). No evident regularity was observed in the adsorption of CHA and MYR because the adsorption of drug molecules is physical without any specific binding. As shown in Figure 9(b), the MIP-MSL and MSL contact lenses exhibited a certain amount of OFL adsorption and reached 2.86 mg/g and 1.44 mg/g, respectively, which could be used for the drug delivery system [39]. Evidently, the adsorption capacity of the MSL contact lenses was significantly lower than that of the MIP-MSL contact lenses.

3.10. Antibacterial Properties. The in vitro antibacterial potential of streptomycin (S_{10}), cefotaxime (CTX_{30}), the MIP-MSL contact lenses, and the MIP/OFL-MSL contact lenses was investigated for positive *S. aureus* and negative *E.coli* through the disc diffusion method [40]. S_{10}, CTX_{30}, and the MIP/OFL-MSL contact lenses (Figures 10(a) (A, B, D) and 10(b) (A, B, D)) expressed an inhibition zone. By contrast, the MIP-MSL contact lenses (Figure 10(a) C and 10(b) C] did not exhibit antibacterial activity. The control S_{10} displayed an inhibition ring size of 18.1 mm and 0 mm for *S. aureus* and *E. coli*, respectively. The control CTX_{30} displayed an inhibition ring size of 22.5 mm and 22.6 mm for *S.*

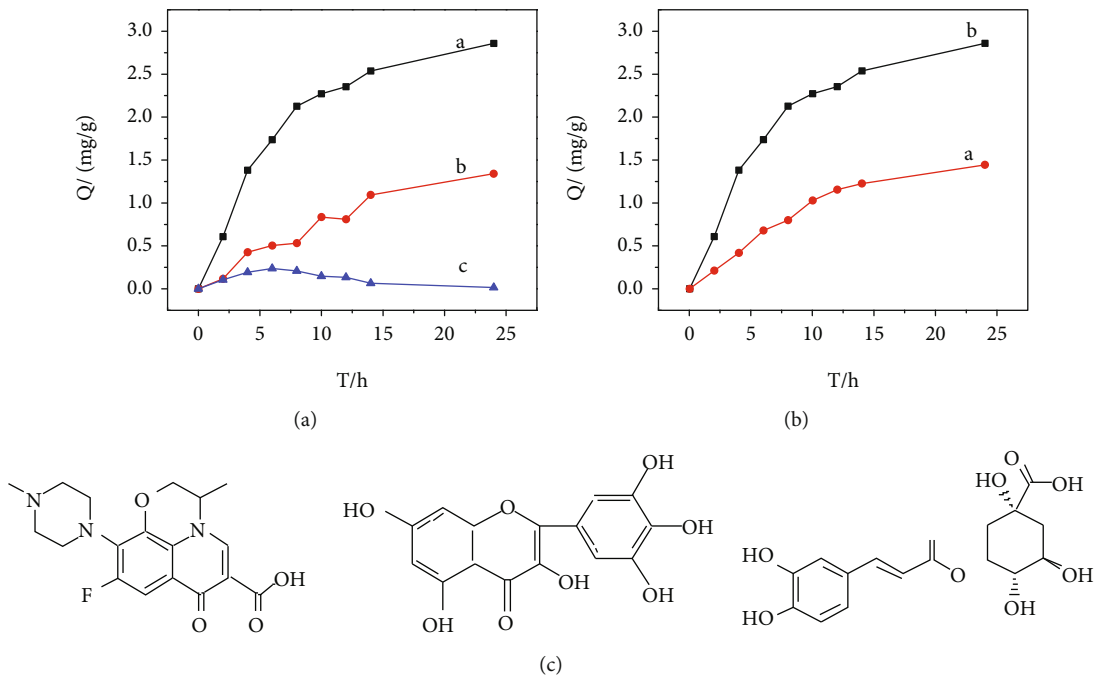

Figure 9: (a) Selective adsorption of the MIP-MSL contact lenses: (A) OFL, (B) MYR, and (C) CHA. (b) Adsorption curves of OFL: (A) MSL and (B) MIP-MSL contact lenses. (c) Structural formula: (A) OFL, (B) MYR, and (C) CHA.

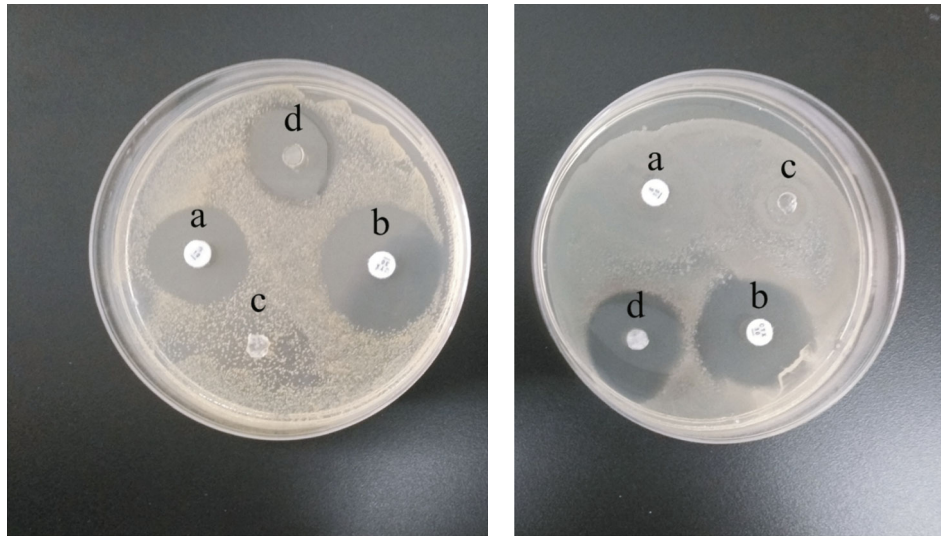

Figure 10: Antibacterial activity screening images of the samples against (a) *S. aureus* and (b) *E. coli*: (A) streptomycin (S_{10}), (B) cefotaxime (CTX_{30}), (C) MIP-MSL contact lenses, and (D) MIP/OFL-MSL contact lenses.

aureus and *E. coli*, respectively. The MIP/OFL-MSL contact lenses presented a growth inhibition ring size of 15.2 mm and 17.8 mm for *S. aureus* and *E. coli*, respectively. In addition, we studied the concentration effect of the OFL on the antibacterial property. It was found that with the concentration of OFL increasing, the MIP/OFL-MSL contact lenses exhibited better antibacterial properties on *S. aureus* and *E. coli*. The good antibacterial activity of the MIP/OFL-MSL contact lenses can be attributed to the efficient release of OFL in the media.

4. Conclusion

NVP was successfully introduced into the synthesis of MSL contact lenses by ultraviolet curing, and the effects of NVP on the structure and properties were investigated. The SEM images exhibited that the addition of NVP resulted in the porous structure of the MSL contact lenses. Compared with the SL contact lenses, the MSL contact lenses had better swelling property of 30.2% at 37°C, light transmittance of 95.06%, and air permeability of 23.7%. The tensile strength

and elongation at break of the MSL contact lenses were 0.649 MPa and 117.75%, respectively. Moreover, the MIP/OFL-MSL contact lenses that can selectively identify OFL were synthesized via free radical polymerization. The selective adsorption and antibacterial properties of the MIP-MSL contact lenses were studied. It was found that the MIP-MSL contact lenses can effectively select and recognize OFL. Meanwhile, the MIP/OFL-MSL contact lenses developed excellent antibacterial properties against *S. aureus* and *E. coli*. The contact lenses exhibit promising application potential in the field of eye disease treatment.

Data Availability

The data used to support the findings of this study are available from the corresponding author upon request.

Conflicts of Interest

The authors declare that they have no conflict of interest.

Acknowledgments

This work was supported by the Natural Science Foundation of China (51902145), the research grants from Six Talent Peaks Project in Jiangsu Province (no. XCL-109), the training objects of young academic leaders of Cyan Engineering in Jiangsu Province, and the Natural Science Foundation of Jiangsu Province (BK20190113).

References

[1] N. Wronska, J. P. Majoral, D. Appelhans, M. Bryszewska, and K. Lisowska, "Synergistic effects of anionic/cationic dendrimers and levofloxacin on antibacterial activities," *Molecules*, vol. 24, no. 16, p. 2894, 2019.

[2] M. Elfiky, N. Salahuddin, A. Hassanein, A. Matsuda, and T. Hattori, "Detection of antibiotic ofloxacin drug in urine using electrochemical sensor based on synergistic effect of different morphological carbon materials," *Microchemical Journal*, vol. 146, pp. 170–177, 2019.

[3] M. H. Al-Jabari, S. Sulaiman, S. Ali, R. Barakat, A. Mubarak, and S. A. Khan, "Adsorption study of levofloxacin on reusable magnetic nanoparticles: kinetics and antibacterial activity," *Journal of Molecular Liquids*, vol. 291, article 111249, 2019.

[4] D. S. Diane, L. Tang, D. L. Schwob, J. I. Usansky, and Y. J. Gordon, "Comparative tear concentrations over time of ofloxacin and tobramycin in human eyes," *Clinical Pharmacology & Therapeutics*, vol. 55, no. 3, pp. 284–292, 1994.

[5] K. Ogawa, M. Hyuga, T. Okada, and N. Minoura, "Development of lipid A-imprinted polymer hydrogels that selectively recognize lipopolysaccharides," *Biosensors & Bioelectronics*, vol. 38, no. 1, pp. 215–219, 2012.

[6] P. B. Morgan, N. Efron, M. Helland et al., "Global trends in prescribing contact lenses for extended wear," *Contact Lens & Anterior Eye*, vol. 34, no. 1, pp. 32–35, 2011.

[7] A. H. Salama, M. M. Abou Samra, G. E. A. Awad, and S. S. Mansy, "Promising bioadhesive ofloxacin-loaded polymeric nanoparticles for the treatment of ocular inflammation: formulation and in vivo evaluation," *Drug Delivery and Translational Research*, vol. 11, no. 5, pp. 1943–1957, 2021.

[8] S. Nuti, J. Fernandez-Lodeiro, D. S. Benedetta et al., "Engineered nanostructured materials for ofloxacin delivery," *Frontiers in Chemistry*, vol. 6, article 554, 2018.

[9] C. O. Dominguez-Godinez, A. Martin-Gil, G. Carracedo, A. Guzman-Aranguez, J. M. González-Méijome, and J. Pintor, "Administracion in vitro e in vivo del secretagogo diadenosin tetrafosfato utilizando lentes de contacto blandas convencionales y de hidrogel de silicona," *Journal of Optometry*, vol. 6, no. 4, pp. 205–211, 2013.

[10] U. Ubani-Ukoma, D. Gibson, G. Schultz, B. O. Silva, and A. Chauhan, "Evaluating the potential of drug eluting contact lenses for treatment of bacterial keratitis using an ex vivo corneal model," *International Journal of Pharmaceutics*, vol. 565, pp. 499–508, 2019.

[11] Y. Li, C. Huang, X. Yang, and X. Zhang, "Ofloxacin laden microemulsion contact lens to treat conjunctivitis," *Journal of Biomaterials Science. Polymer Edition*, vol. 31, no. 12, pp. 1566–1579, 2020.

[12] H. M. Eid, M. H. Elkomy, S. F. El Menshawe, and H. F. Salem, "Development, optimization, and in vitro/in vivo characterization of enhanced lipid nanoparticles for ocular delivery of ofloxacin: the influence of pegylation and chitosan coating," *American Association of Pharmaceutical Scientists Pharm SciTech*, vol. 20, no. 5, 2019.

[13] D. Lee, N. Lee, and I. Kwon, "Efficient loading of ophthalmic drugs with poor loadability into contact lenses using functional comonomers," *Biomaterials Science*, vol. 6, no. 10, pp. 2639–2646, 2018.

[14] Y. Matsuzaki, H. Toshida, T. Ohta, and A. Murakami, "A case of atypical mucin balls wearing extended wear of silicone hydrogel lens for therapeutic use," *Case reports in ophthalmological medicine*, vol. 2013, Article ID 167854, 2013.

[15] N. García-Porta, L. Rico-del-Viejo, H. Ferreira-Neves, S. C. Peixoto-de-Matos, A. Queirós, and J. M. González-Méijome, "Performance of three multipurpose disinfecting solutions with a silicone hydrogel contact lens," *BioMed Research International*, vol. 2015, Article ID 216932, 2015.

[16] P. C. Nicolson and J. Vogt, "Soft contact lens polymers: an evolution," *Biomaterials*, vol. 22, no. 24, pp. 3273–3283, 2002.

[17] K. Ishihara, K. Fukazawa, V. Sharma et al., "Antifouling silicone hydrogel contact lenses with a bioinspired 2-methacryloyloxyethyl phosphorylcholine polymer surface," *ACS Omega*, vol. 6, no. 10, pp. 7058–7067, 2021.

[18] C.-C. Peng, M. T. Burke, and A. Chauhan, "Transport of topical anesthetics in vitamin E loaded silicone hydrogel contact lenses," *Langmuir*, vol. 28, pp. 1478–1487, 2012.

[19] J. Wang, S. Xi, B. Wang, Z. Chen, K. Zheng, and X. Zhou, "Clinical observation of silicon hydrogel contact lens fitted immediately after small incision lenticule extraction (SMILE)," *Journal of Ophthalmology*, vol. 2020, Article ID 2604917, 2020.

[20] L. Chen, X. Wang, W. Lu, X. Wu, and J. Li, "Molecular imprinting: perspectives and applications," *Chemical Society Reviews*, vol. 45, no. 8, pp. 2137–2211, 2016.

[21] P. B. Morgan, N. Efron, M. Helland et al., "Twenty first century trends in silicone hydrogel contact lens fitting: an international perspective," *Contact Lens & Anterior Eye*, vol. 33, no. 4, pp. 196–198, 2010.

[22] J. Dolai, H. Ali, and N. R. Jana, "Molecular imprinted polycyclodextrin for selective removal of dibutyl phthalate," *ACS Applied Polymer Materials*, vol. 2, no. 2, pp. 691–698, 2020.

[23] C. Jantarat, K. Attakitmongkol, S. Nichsapa, P. Sirathanarun, and S. Srivaro, "Molecularly imprinted bacterial cellulose for sustained-release delivery of quercetin," *Journal of Biomaterials Science. Polymer Edition*, vol. 31, no. 15, pp. 1961–1976, 2020.

[24] M. J. Shin, M. Kim, and J. S. Shin, "Switchable cholesterol recognition system with Diels–Alder reaction using molecular imprinting technique on self-assembled monolayer," *Polymer International*, vol. 68, no. 10, pp. 1722–1728, 2019.

[25] A. Tieppo, C. J. White, A. C. Paine, M. L. Voyles, M. K. McBride, and M. E. Byrne, "Sustained in vivo release from imprinted therapeutic contact lenses," *Journal of Controlled Release*, vol. 157, no. 3, pp. 391–397, 2012.

[26] J. Tavakoli, H. P. Zhang, B. Z. Tang, and Y. Tang, "Aggregation-induced emission lights up the swelling process: a new technique for swelling characterisation of hydrogels," *Materials Chemistry Frontiers*, vol. 3, no. 4, pp. 664–667, 2019.

[27] JAMA, "Drugs for some common eye disorders," *Treatment Guidelines from the Medical Letter*, vol. 10, no. 123, pp. 79–86, 2012.

[28] M. Korogiannaki, M. Samsom, T. A. Schmidt, and H. Sheardown, "Surface-functionalized model contact lenses with a bioinspired proteoglycan 4 (PRG4)-grafted layer," *ACS Applied Materials & Interfaces*, vol. 10, no. 36, pp. 30125–30136, 2018.

[29] H. Edwards and A. F. Johnson, "A Raman spectroscopic study of N, N-dimethylacrylamide," *Spectrochimica Acta Part A Molecular Spectroscopy*, vol. 50, no. 2, pp. 255–261, 1994.

[30] Y. Y. Wei, S. S. An, S. Sun, and Y. Jiang, "Photo-polymerized and thermal-polymerized silicon hydrogels with different surface microstructure and wettability," *Colloids and Surfaces A: Physicochemical and Engineering Aspects*, vol. 618, article 126284, 2021.

[31] M. Lira, C. Lourenco, M. Silva, and G. Botelho, "Estabilidad fisicoquimica de los materiales de las lentes de contacto, para aplicaciones biomedicas," *Journal of Optometry*, vol. 13, no. 2, pp. 120–127, 2020.

[32] M. Lin, Q. Zhao, S. Dang, Z. Yang, Z. Dong, and J. Zhang, "Temperature resistance of AM/AMPS/NVP copolymer microspheres," *Iranian Polymer Journal*, vol. 29, no. 5, pp. 445–453, 2020.

[33] T. Shen, S. Mao, F. Ding, T. Han, and M. Gao, "Selective adsorption of cationic/anionic tritoluene dyes on functionalized amorphous silica: a mechanistic correlation between the precursor, modifier and adsorbate," *Colloids and Surfaces A: Physicochemical and Engineering Aspects*, vol. 618, article ???, 2021.

[34] N. S. Malik, M. Ahmad, M. U. Minhas, G. Murtaza, and Q. Khalid, "Polysaccharide hydrogels for controlled release of acyclovir: development, characterization and in vitro evaluation studies," *Polymer Bulletin*, vol. 74, no. 10, pp. 4311–4328, 2017.

[35] M. Kubbinga, M. A. Nguyen, P. Staubach, S. Teerenstra, and P. Langguth, "The influence of chitosan on the oral bioavailability of acyclovir—a comparative bioavailability study in humans," *Pharmaceutical Research*, vol. 32, no. 7, pp. 2241–2249, 2015.

[36] D. Rahangdale, A. Kumar, G. Archana, and R. S. Dhodapkar, "Ion cum molecularly dual imprinted polymer for simultaneous removal of cadmium and salicylic acid," *Journal of Molecular Recognition*, vol. 31, no. 3, p. e2630, 2018.

[37] M. Korogiannaki, L. Jones, and H. Sheardown, "Impact of a hyaluronic acid-grafted layer on the surface properties of model silicone hydrogel contact lenses," *Langmuir*, vol. 35, no. 4, pp. 950–961, 2019.

[38] M. Vivero-Lopez, A. Muras, D. Silva et al., "Resveratrol-loaded hydrogel contact lenses with antioxidant and antibiofilm performance," *Pharmaceutics*, vol. 13, no. 4, p. 532, 2021.

[39] F. S. C. Rodrigues, A. Campos, J. Martins, A. F. Ambrosio, and E. J. Campos, "Emerging trends in nanomedicine for improving ocular drug delivery: light-responsive nanoparticles, mesoporous silica nanoparticles, and contact lenses," *ACS Biomaterials Science & Engineering*, vol. 6, no. 12, pp. 6587–6597, 2020.

[40] M. G. Hewitt, P. W. J. Morrison, H. M. Boostrom et al., "In vitro topical delivery of chlorhexidine to the cornea: enhancement using drug-loaded contact lenses and β-cyclodextrin complexation, and the importance of simulating tear irrigation," *Molecular Pharmaceutics*, vol. 17, no. 4, pp. 1428–1441, 2020.